



The effect of oxygen vacancies on the electronic phase transition in $\text{La}_{1/3}\text{Sr}_{2/3}\text{FeO}_3$ films

Rebecca J. Sichel-Tissot,¹ Robert C. Devlin,¹ Philip J. Ryan,² Jong-Woo Kim,² and Steven J. May¹

¹Department of Materials Science and Engineering, Drexel University, Philadelphia, Pennsylvania 19104 USA

²X-ray Science Division, Argonne National Laboratory, Argonne, Illinois 60439 USA

(Received 13 September 2013; accepted 10 November 2013; published online 22 November 2013)

Synchrotron x-ray diffraction and electrical resistivity were used to probe the electronic phase transition in two strained $\text{La}_{1/3}\text{Sr}_{2/3}\text{FeO}_3$ films on (001) SrTiO_3 substrates, one nominally stoichiometric and one with a higher concentration of oxygen vacancies. We present evidence that oxygen vacancies inhibit the size of charge ordered domains and reduce the abruptness of the phase transition. Additionally, the correlation lengths measured from (4/3 4/3 4/3) peaks, arising from charge disproportionation, increase rapidly across the transition, suggesting that the resistivity increase at the transition temperature is caused by the nucleation and growth of charge ordered domains. © 2013 AIP Publishing LLC. [<http://dx.doi.org/10.1063/1.4833276>]

There is growing interest in understanding and controlling abrupt electronic phase transitions in complex oxide heterostructures as a platform for ultrafast, low power electronics.¹ Iron-based perovskites, such as $\text{La}_{1/3}\text{Sr}_{2/3}\text{FeO}_3$ (LSFO), can exhibit a first order phase transition leading to an abrupt increase in resistivity,^{2–5} making ferrites potential candidates for applications based on electronic transitions. In bulk LSFO, the transition occurs around 195 K, with the low temperature insulating state commonly attributed to a magnetically induced charge ordered phase in which a nominal $\text{Fe}^{3.67-\delta}-\text{Fe}^{3.67-\delta}-\text{Fe}^{3.67+2\delta}$ arrangement or a similar pattern of ordered ligand holes is stabilized along the [111] direction.^{6–9}

Despite the previous research published on the phase transition in bulk and thin film LSFO, there are still questions regarding the nature of the phase transition and the electronic transport properties. X-ray absorption and photoelectron emission spectra of LSFO suggest that transition-induced changes to the electronic structure take place gradually over ~ 100 K.¹⁰ Similarly, optical absorption measurements revealed a continual increase in the band gap from 198 to ~ 100 K.¹¹ This contrasts with the electronic transport, which clearly shows a discontinuity in resistivity over just a few degrees.³ However, the abruptness of the transition varies from report to report—with studies reporting behavior ranging from an increase in the resistivity by an order of magnitude^{2,12} to a simple change in the slope.⁹ What is the origin of this variation in the reported transport properties of LSFO? The electrical properties of ferrites and other perovskites are highly sensitive to oxygen vacancies,¹³ so we hypothesized that variations in LSFO conductivity arise from differing degrees of oxygen content.

In order to learn how oxygen vacancies affect the charge ordering phase transition, we have characterized the electronic behavior of LSFO thin films with different oxygen contents. The effects of oxygen on the transport properties were measured using the four-point probe method. X-ray diffraction was used to probe the modulation of charge along the [111] as a function of temperature. Analysis of superstructure reflections yielded measurements of the correlation

length of charge ordered regions. By comparing the resistivity, correlation lengths, and integrated intensity of the reflections, we observed two components to the phase transition—nucleation and growth of charge ordered regions near T^* , and a gradual increase of integrated intensity, which is consistent with increasing disproportionation well below T^* . Oxygen vacancies increase the resistivity at all temperatures measured and decrease the maximum correlation length. In contrast, the vacancies appear to have a minimal effect on the transition temperature, ordering wavevector, or how quickly charge ordered regions initially expand below the transition.

Thin films of LSFO were deposited on SrTiO_3 (STO) (001) single crystal substrates using oxide molecular beam epitaxy (Omicron Nanotechnology GmbH LAB-10 system). Bulk LSFO has a pseudocubic lattice parameter of 3.871 Å;^{5,14} thus, the biaxial strain state of the film is 0.9%. The films were grown in a mixture of oxygen and ozone ($\sim 95:5 \text{ O}_2:\text{O}_3$) at a pressure of 8×10^{-6} Torr. Deposition rates of elemental sources were monitored using a quartz crystal monitor and calibrated from Rutherford backscattering measurements of films grown concurrently on MgO. We estimate the uncertainty in cation stoichiometry to be ± 0.03 . Substrate temperatures were kept between 575° and 600 °C. The surface structure of the film was monitored using reflection high energy electron diffraction (RHEED) during the growth. The structure and electronic properties of the LSFO thin films were characterized using x-ray diffraction, x-ray reflectivity, and resistivity measurements. In the synchrotron measurements, LSFO thin films were mounted in a cryostat on a Huber six circle diffractometer¹⁵ to enable grazing-incidence diffraction at low temperatures. For the 41 u.c. sample, we used an incident angle 0.1° above the critical angle to maximize scattering from the film for the low temperature diffraction measurements. Electronic transport measurements were performed using a Keithley 6220 current source and 2182A nanovoltmeter with the sample in a Quantum Design Physical Properties Measurement System and a custom built immersion transport setup. Films were contacted with silver paint and

measured in the four point probe geometry. As-grown films were found to be oxygen deficient based on c -axis parameters and resistivity values, both of which increase with increasing oxygen deficiency. A post-growth anneal in flowing oxygen at 675 °C for 4 h was found to reduce the anion deficiency in the films as evidenced by a reduction in c -axis parameter and decrease in resistivity. Over a time scale of months, the films tend to lose oxygen. The 86 u.c. film in this study was measured three months after it was annealed. We believe this to be the origin of the higher relative concentration of vacancies in this film compared to the 41 u.c. film, which was measured 10 days after its anneal.

Synchrotron x-ray diffraction experiments were conducted at Sector 6-ID-B of the Advanced Photon Source using a photon energy of 12.4 keV. Figure 1 shows scans along the [00L] direction across the substrate and film (002) reflections at 300 K. The oscillations in intensity are caused by the finite thickness of the film. Scans across the LSF0 (112) and (111) confirm that the films have the same in-plane lattice parameters as the substrate and remain coherently strained. The [00L] scans were fit by simulating the diffracted intensity using GenX.¹⁶ The resulting thicknesses and lattice parameters are shown in Fig. 1. The larger lattice constant of the 86 unit cell (u.c.) thick film is attributed to a higher concentration of oxygen vacancies than the thinner 41 u.c. film.^{17,18} We note that oxygen vacancy concentration affects the volume of the unit cell and the bulk lattice parameters, as oxygen vacancies expand the lattice. Since the strain in the film depends on the bulk and film lattice parameters, the two films have slightly different strain states despite having identical in-plane lattice parameters. Therefore, efforts to

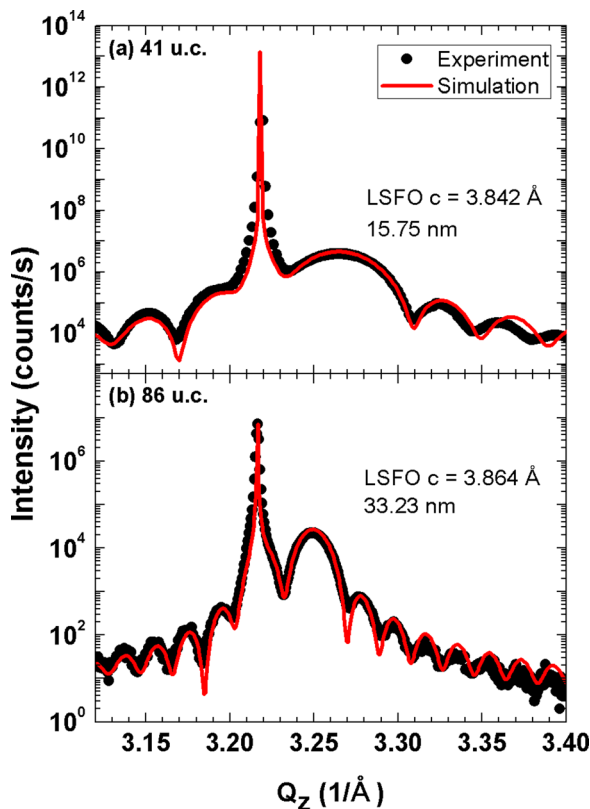


FIG. 1. X-ray diffraction and simulations of (a) 41 u.c. and (b) 86 u.c. of LSF0 on (001) STO.

isolate the effects of vacancies cannot be completely decoupled from the resultant changes in epitaxial strain.

The electronic transport properties were measured to confirm the presence of the phase transition. Figure 2(a) shows the resistivity as a function of temperature for both films. The room temperature resistivity of the 86 u.c. film is 0.0034 Ω -cm, compared to 0.0018 Ω -cm in the 41 u.c. film. The larger resistivity in the 86 u.c. film is also consistent with a higher concentration of oxygen vacancies relative to the 41 u.c. film, as previous studies of bulk $\text{La}_{1-x}\text{Sr}_x\text{FeO}_{3-\delta}$ have clearly demonstrated that resistivity increases with increasing δ .^{13,19} Near 190 K, the films exhibit a jump in resistivity indicative of the phase transition as LSF0 goes from a poorly conducting to an insulating state. The transition is abrupt for the 41 u.c. film, but is broader for the oxygen deficient 86 u.c. film (Fig. 2(a)). In order to consistently define the transition temperature (T^*) and the range of temperatures (ΔT) over which the transition has the largest effect on the resistivity, we examined the first and second derivatives of the resistivity with respect to temperature. We define T^* to be the maximum of the second derivative, $d^2 \log(\rho)/dT^2$. T^* is 186.5 K for the 41 u.c. film and 186 K for the 86 u.c. film. This also serves as the high temperature of the transition range. The low temperature of the transition range is defined to be the minimum of the first derivative. Figure 2(b) shows the derivatives for the 41 u.c. film and a blue box that highlights ΔT . Figure 2(c) shows the same analysis for the 86 u.c. film. ΔT is 5 K and 6 K for the 41 and 86 u.c. films, respectively. The maximum value of $d^2 \log(\rho)/dT^2$ serves as a better measure of the abruptness of the transition as it takes into account the magnitude of resistivity change at the transition. The second derivative is three

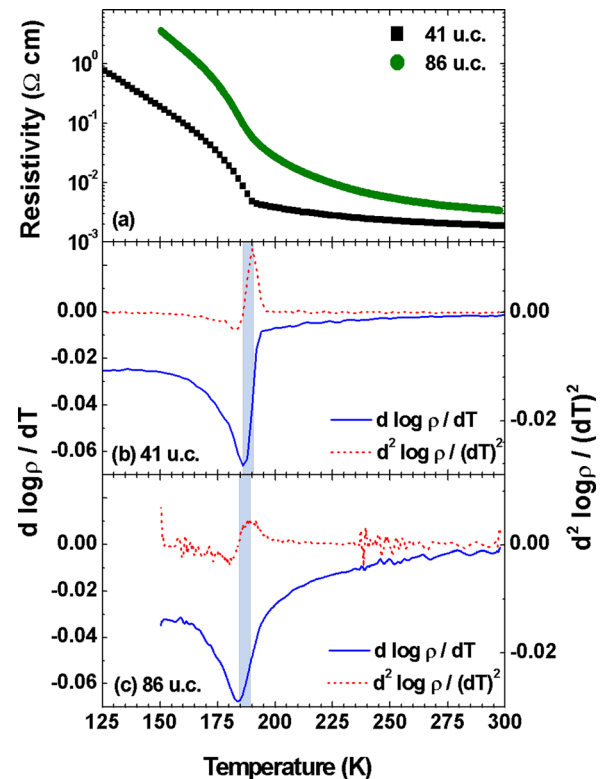


FIG. 2. Resistivity as a function of temperature for the two LSF0 films (a); derivatives of resistivity with respect to temperature (b) and (c).

times larger in the 41 u.c. film than to the 86 u.c. film. While the abruptness of the transition is dependent on the vacancy concentration, T^* is nearly identical in the two films. We note that seven LSFO/STO samples of different thicknesses and oxygen content were measured, and in all of these films T^* was between 185 K and 195 K, again consistent with the observation that the transition temperature is not strongly dependent on the vacancy concentration.

We used synchrotron XRD to confirm that the electronic phase transition is caused by charge ordering, as in bulk LSFO. Previous studies have found a charge modulation along the pseudocubic [111].^{8,9,20} We observe a reflection at the $(4/3\ 4/3\ 4/3)$ of the film which appears below T^* . Figure 3 shows L scans through the $(4/3\ 4/3\ 4/3)$ at several different temperatures for both samples. The reflection appears as the samples are cooled below T^* and increases in intensity as the samples are cooled further. The tensile strain in the films does not change the charge ordering wavevector direction or periodicity. We note that we have also measured strained LSFO films on $(\text{La,Sr})(\text{Al,Ta})\text{O}_3$ (LSAT) and DyScO_3 (110) substrates and have observed that the charge ordering remains along the [111] direction for these films as well.

The intensity and width of the charge ordering reflection provides information about the disproportionation and correlation length of charge ordered regions. Scans across the $(4/3\ 4/3\ 4/3)$ peaks along the [00L] and [H00] were fit to Lorentzian functions to measure the out-of-plane and in-plane correlation lengths, respectively. The integrated

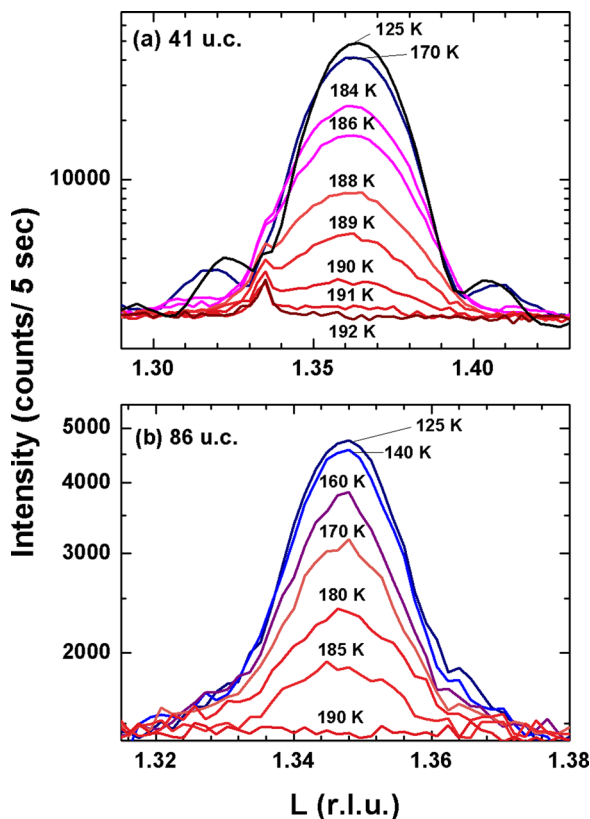


FIG. 3. The $(4/3\ 4/3\ 4/3)$ reflection from (a) 41 u.c. and (b) 86 u.c. films. Above the transition temperature, T^* , no reflection is observed. The small, sharper peak in (a) at $L = 1.335$ comes from a higher harmonic x-ray diffracting from the substrate. The reciprocal lattice units are given with respect to the SrTiO_3 substrate.

intensity was measured using the fit to the [00L] scans. The correlation lengths, a measure of the average domain size of charge ordered regions, were determined from $1/\text{FWHM}$. Figure 4 shows the integrated intensity and correlation lengths as a function of temperature. Blue boxes indicate the transition regions shown in Figure 2. The out-of-plane correlation length, ξ_L , in the 41 u.c. film is limited to a maximum at the film thickness, 157 Å. In the 86 u.c. film, ξ_L has a maximum of 248 Å, well below the film thickness of 332 Å. The in-plane correlation length, ξ_H , in the oxygen deficient 86 u.c. film (Fig. 4(b)) is less than the more stoichiometric film.

We compared the resistivity and the correlation lengths as a function of temperature to learn more about the microscopic details of the phase transition. Within ΔT , the correlation lengths increase rapidly to $\sim 85\%$ of the saturated values, suggesting that the expansion of the insulating charge ordered domains plays a key role in the resistivity increase over this temperature range.

While the correlation lengths saturate at certain maximum values, the integrated intensity shows a different behavior. The intensity increases as the sample is cooled, but does not appear to reach a saturation point within the measured temperature range from 125 K to 190 K. The integrated intensity from the oxygen deficient sample increases more slowly compared to the more stoichiometric, 41 u.c. film. X-ray absorption spectroscopy and infrared absorption studies found shifts in the O 2p spectra and increases in the band gap continue well below the transition temperature.^{10,11,21} Consequently, we propose that the phase transition takes place in two stages. At temperatures just below T^* , the rising correlation lengths show that charge ordered domains nucleate and expand rapidly with respect to temperature. The

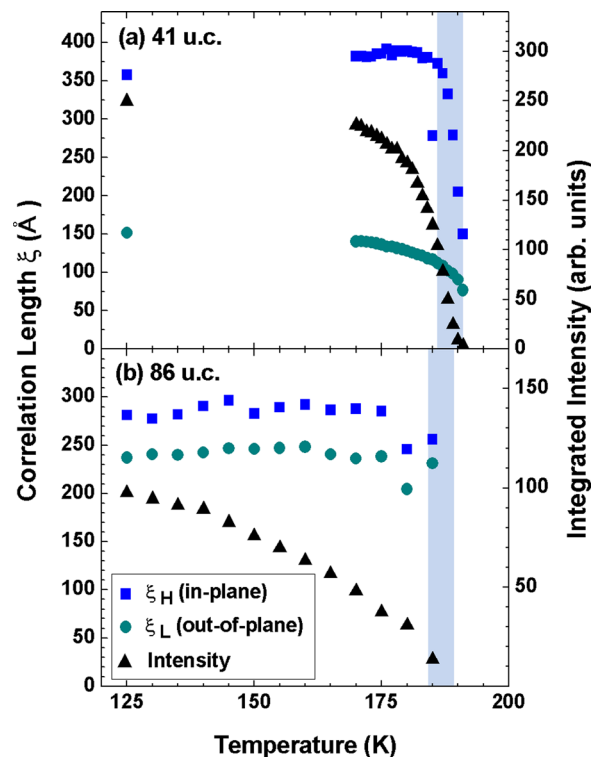


FIG. 4. Correlation lengths and integrated intensity of the $(4/3\ 4/3\ 4/3)$ reflection from the (a) 41 u.c. and (b) 86 u.c. films.

resistivity jump is caused by an increasing volume fraction of the film that is charge ordered, and therefore more insulating. Upon further cooling, the magnitude of the disproportionation gradually increases as suggested by XAS. A larger disproportionation would increase the structure factor of the (4/3 4/3 4/3), which would explain the increased intensity and constant correlation lengths.

In summary, we have studied epitaxial (001) LSFO/STO thin films with different oxygen vacancy concentrations to probe the effects of oxygen stoichiometry on the electronic phase transition. The transition temperature and the abruptness of the transition were measured using resistivity and compared to an x-ray reflection arising from a charge modulation along the [111]. Our results show that oxygen content strongly affects the charge ordering transition in LSFO. The oxygen deficient sample has a broader transition, larger resistivity in the conducting state, and the integrated intensity exhibits a much more gradual increase over the measured temperature range, as compared to the thinner, more stoichiometric film. We find that the oxygen vacancies do not affect the rate of nucleation and initial growth of charge ordering domains, but do decrease their correlation length. Our results also suggest that the phase transition takes place in two steps—rapid domain nucleation and growth near the transition temperature and a more gradual process that is affected by oxygen stoichiometry. Comparisons of the resistivity and correlation lengths indicate that the initial increase in resistivity below T^* is caused by the nucleation and expansion of charge ordered domains. The integrated intensity continues to increase well after the domains have ceased expanding, consistent with a continual increase in the magnitude of disproportionation.

This work was supported by Office of Naval Research under Grant No. N00014-11-1-0664. Use of the Advanced Photon Source, an Office of Science User Facility operated

for the U.S. Department of Energy (DOE) Office of Science by Argonne National Laboratory, was supported by the U.S. DOE under Contract No. DE-AC02-06CH11357.

- ¹Z. Yang, C. Ko, and S. Ramanathan, *Annu. Rev. Mater. Res.* **41**, 337 (2011).
- ²S. K. Park, T. Ishikawa, and Y. Tokura, *Phys. Rev. B* **60**, 10788 (1999).
- ³J. Matsuno, T. Mizokawa, A. Fujimori, Y. Takeda, S. Kawasaki, and M. Takano, *Phys. Rev. B* **66**, 193103 (2002).
- ⁴T. Takeda, R. Kanno, Y. Kawamoto, M. Takano, S. Kawasaki, T. Kamiyama, and F. Izumi, *Solid State Sci.* **2**, 673 (2000).
- ⁵W. Prellier and B. Mercey, *J. Phys. D: Appl. Phys.* **35**, L48 (2002).
- ⁶P. D. Battle, T. C. Gibb, and P. Lightfoot, *J. Solid State Chem.* **84**, 271 (1990).
- ⁷R. J. McQueeney, J. Ma, S. Chang, J.-Q. Yan, M. Hehlen, and F. Trouw, *Phys. Rev. Lett.* **98**, 126402 (2007).
- ⁸J. Herrero-Martin, G. Subias, J. Garcia, J. Blasco, and M. C. Sánchez, *Phys. Rev. B* **79**, 045121 (2009).
- ⁹J. Okamoto, D. J. Huang, K. S. Chao, S. W. Huang, C.-H. Hsu, A. Fujimori, A. Masuno, T. Terashima, M. Takano, and C. T. Chen, *Phys. Rev. B* **82**, 132402 (2010).
- ¹⁰H. Wadati, A. Chikamatsu, R. Hashimoto, M. Takizawa, H. Kumigashira, A. Fujimori, M. Oshima, M. Lippmaa, M. Kawasaki, and M. Koinuma, *J. Phys. Soc. Jpn.* **75**, 054704 (2006).
- ¹¹T. Ishikawa, S. K. Park, T. Katsufuji, T. Arima, and Y. Tokura, *Phys. Rev. B* **58**, R13326 (1998).
- ¹²K. Ueno, A. Ohtomo, F. Sato, and M. Kawasaki, *Phys. Rev. B* **73**, 165103 (2006).
- ¹³T. Maeder and Bednorz, *J. Eur. Ceram. Soc.* **19**, 1507 (1999).
- ¹⁴J. Blasco, M. C. Sánchez, J. García, J. Stankiewicz, and J. Herrero-Martin, *J. Cryst. Growth* **310**, 3247 (2008).
- ¹⁵H. You, *J. Appl. Cryst.* **32**, 614 (1999).
- ¹⁶M. Björck and G. Andersson, *J. Appl. Crystallogr.* **40**, 1174 (2007).
- ¹⁷Y.-M. Kim, J. He, M. D. Biegalski, H. Ambaye, V. Lauter, H. M. Christen, S. T. Pantelides, S. J. Pennycook, S. V. Kalinin, and A. Y. Borisevich, *Nature Mater.* **11**, 888 (2012).
- ¹⁸X. Chen, J. Yu, and S. B. Adler, *Chem. Mater.* **17**, 4537 (2005).
- ¹⁹H. D. Zhou and J. B. Goodenough, *J. Solid State Chem.* **178**, 3679 (2005).
- ²⁰J. Q. Li, Y. Matsui, S. K. Park, and Y. Tokura, *Phys. Rev. Lett.* **79**, 297 (1997).
- ²¹H. Wadati, D. Kobayashi, H. Kumigashira, K. Okazaki, T. Mizokawa, A. Fujimori, K. Horiba, M. Oshima, N. Hamada, M. Lippmaa, M. Kawasaki, and H. Koinuma, *Phys. Rev. B* **71**, 035108 (2005).